Acta Cryst E CRYSTALLOGRAPHIC COMMUNICATIONS

ISSN 2056-9890

N,*N*′-Dibenzylethylenediammonium dichloride

Mary Helene Marmande,[a] Bailey N. Baxter,[a] Matthias Zeller[b] and David C. Forbes[a]*

[a]University of South Alabama, Department of Chemistry, 6040 USA Drive South, Mobile, Alabama 36608, USA, and [b]Purdue University, Department of Chemistry, 560 Oval Drive, West Lafayette, Indiana 47907, USA. *Correspondence e-mail: dforbes@southalabama.edu

Received 29 August 2024
Accepted 27 September 2024

Edited by D. R. Manke, University of Massachusetts Dartmouth, USA

Keywords: crystal structure; side reaction; hydrogen bonding; pseudo-translation; modulation.

CCDC reference: 2387167

Supporting information: this article has supporting information at journals.iucr.org/e

The isolation and crystalline structure of *N*,*N*′-dibenzylethylenediammonium dichloride, $C_{16}H_{22}N_2^{2+}\cdot 2Cl^-$, is reported. This was obtained as an unintended product of an attempted Curtius rearrangement that involved benzylamine as one of the reagents and 1,2-dichloroethane as the solvent. Part of a series of reactions of a course-based undergraduate research experience (CURE), this was not the intended reaction outcome. The goal of the course was to engage students as active participants in a laboratory experience which applies the foundational techniques of a synthetic organic laboratory, using the Curtius rearrangement as a tool for the assembly of medicinally significant scaffolds. The isolation of the title compound, *N*,*N*′-dibenzylethylenediammonium dichloride, the result of the 1,2-dichloroethane solvent outcompeting the Curtius isocyanate intermediate in the reaction with the nucleophilic amine, confirms the importance of conducting research at the undergraduate level where the outcome is not predetermined. The solid-state structure of *N*,*N*′-dibenzylethylenediammonium dichloride was found to feature an all-*trans* methylene-ammonium backbone. Strong N—H···Cl hydrogen bonds and C—H···Cl interactions lead to a layered structure with pseudo-translational symmetry emulating a *C*-centered setting. Different phenyl torsion angles at each end of the molecule enable a more stable packing by allowing stronger hydrogen-bonding interactions, leading to a more ordered but lower symmetry and modulated structure in $P2_1/n$.

1. Chemical context

Research is, by definition, the search for answers to scientific questions for which the answers are not yet known. Traditional classroom teaching does not reflect this well, often focusing on textbook examples with a predetermined outcome. Course-based undergraduate research experiences (CUREs) are research experiences embedded into a formal laboratory course, providing a way for students to experience the process of conducting authentic scientific research (Brownell & Kloser, 2015). The essence of this approach to undergraduate teaching is that students work on research problems with no predetermined answers that go beyond teaching textbook chemistry and that are relevant in the 'outside world' beyond the classroom (Watts & Rodriguez, 2023). Using this approach, we conducted a course with the goal of engaging students as active participants in a laboratory experience, which applies the foundational techniques of a synthetic organic laboratory to the assembly of medicinally significant scaffolds, using the example of the Curtius rearrangement.

The Curtius rearrangement is a well-established and convenient reaction to convert carboxylic acid derivatives *via* their acyl azide to isocyanates (Curtius, 1890, 1894). Depending on the reaction workup, these can be converted

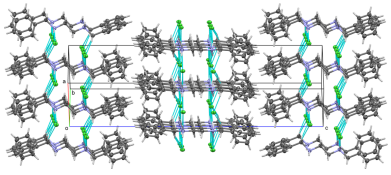

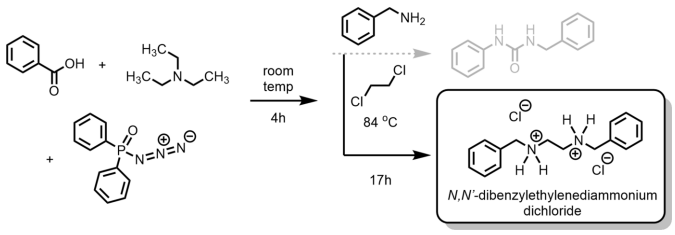

Figure 1
The synthesis showing the intended product (top) and the product actually formed (bottom).

into various amines and their derivatives such carbamates (when treated with alcohols), or urea derivatives (when trapped with an amine). The conversion to the isocyanate requires heating, thus a high boiling solvent is usually required to bring the reaction to completeness. Its tolerance of a wide range of functional groups and complete retention of stereochemistry has made the Curtius rearrangement an attractive route towards various medicinally relevant compounds and drugs, such as *e.g.* Sorafenib or Tamiflu (Ghosh *et al.*, 2018). Diphenylphosphoryl azide (DPPA) is a readily available and easy to use azide source for the Curtius rearrangement (Ninomiya *et al.*, 1974).

In a 2015 article, Reddy and coworkers (Reddy *et al.*, 2015) described the use of this reaction for the synthesis of a series of urea derivatives by treating various benzoic acids with DPPA and triethyl amine as a base. Addition of an aromatic amine and heating in 1,2-dichloroethane (b.p. 356 K) brought the reaction to completeness. Following this literature example, we used benzoic acid with diphenylphosphoryl azide (DPPA) in the presence of benzylamine and triethyl amine with the anticipated outcome being the Curtius rearranged adduct *N*-benzyl-*N*′-phenylurea (Fig. 1). Our goal was to develop a unified approach toward the assembly of carboxylic acid derivatives to serve as advanced scaffolds earmarked toward the preparation of next-generation lipid-like nanoparticles (LLNPs; Hou *et al.*, 2021) using as the key reagent DPPA and as the key step the Curtius rearrangement. To widen the scope of the reaction, we modified the substrates employed to use not only aryl but also alkyl amines. When using aniline derivatives, Reddy and coworkers (Reddy *et al.*, 2015) reported on the formation and screening of 10 urea derivatives. What was not reported was the isolation (or formation) of side products. With our choice of amine (benzylamine *vs* aniline derivatives), however, the expected product *N*-benzyl-*N*′-phenylurea was not observed based upon GCMS analysis of the crude reaction mixture. Isolation of the major reaction product and crystallization allowed for the unambiguous identification of the actual reaction product by single crystal X-ray diffraction, and it was found to be *N*,*N*′-dibenzylethylenediammonium dichloride, the product of the reaction of the strong nucleophile benzylamine with the solvent, 1,2-dichloroethane, outcompeting the reaction of the amine with the isocyanate (Fig. 1). The obvious solution to avoid this undesired reaction outcome was substituting the solvent. Upon switching from 1,2-dichloroethane to acetonitrile, preliminary results indicate formation of the intended carboxylic acid derivatives.

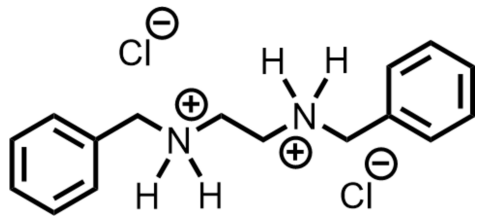

2. Structural commentary

While the outcome of the reaction and formation of *N*,*N*′-dibenzylethylenediammonium dichloride was unexpected, so was the finding that the solid-state structure of this rather simple and basic compound had not been determined previously. Its free base, dibenzylethylenediamine, is a common reagent frequently used as a ligand for the formation of various metal complexes. The structure of its nitrate salt has been reported (CSD entry AFIKEG; Liu *et al.*, 2007), as well as several other salts with more esoteric anions, and also about two dozen metal complexes incorporating it as a ligand are known. The structure of the chloride – or bromide or iodide – is, however, not known. A possible explanation for this unexpected absence of crystal structure data might be the way we experienced this material to crystallize. Crystals obtained by vapor diffusion of ethanol into an aqueous solution of the salt yielded mostly highly twinned multi-domain thin plates and flakes. Diffraction patterns from these larger not-single crystallites tended to emulate a wrong crystal system and space group. Careful examination and screening of crystals revealed a few better-behaved crystallites that were amenable towards analysis by single crystal diffraction, allowing for unambiguous identification of the material. Purity of bulk material was confirmed by ^{1}H and ^{13}C NMR spectroscopy, which matched data previously reported for *N*,*N*′-dibenzylethylenediammonium dichloride (Asadi *et al.*, 2005).

Crystals were found to be monoclinic primitive, in space group $P2_1/n$ with Z = 4. The molecules exhibit no crystallographic symmetry in the solid state, with the two halves of the cation being crystallographically independent. In the solid

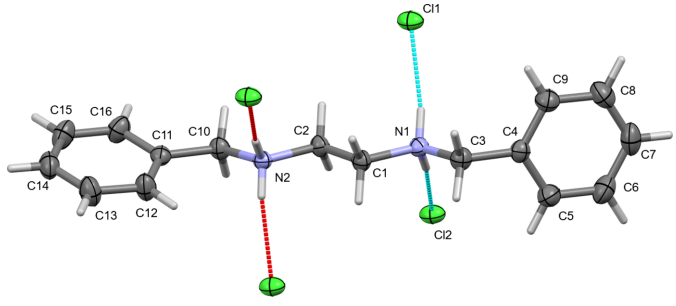

Figure 2
The title compound with the atom-labelling scheme and 50% probability ellipsoids. Unlabeled chloride anions are symmetry equivalent [1 − *x*, 2 − *y*, 1 − *z* for Cl1 (top), −*x*, 1 − *y*, 1 − *z* for Cl2 (bottom)].

Table 1
Hydrogen-bond geometry (Å, °).

D—H···A	D—H	H···A	D···A	D—H···A
N1—H1C···Cl1	0.893 (16)	2.187 (16)	3.0675 (10)	168.6 (13)
N1—H1D···Cl2	0.908 (17)	2.189 (17)	3.0913 (10)	172.7 (13)
N2—H2C···Cl2^{i}	0.867 (16)	2.213 (16)	3.0730 (10)	171.7 (13)
N2—H2D···Cl1^{ii}	0.881 (17)	2.213 (17)	3.0893 (10)	172.9 (13)
C1—H1A···Cl1^{ii}	0.99	2.95	3.7125 (12)	135
C1—H1B···Cl2^{i}	0.99	2.94	3.7000 (12)	135
C2—H2A···Cl1	0.99	2.98	3.7213 (12)	133
C2—H2B···Cl2	0.99	2.97	3.7251 (12)	134
C3—H3A···Cl1^{iii}	0.99	2.65	3.6296 (13)	171
C3—H3B···Cl2^{iv}	0.99	2.71	3.6106 (13)	151
C10—H10A···Cl1^{v}	0.99	2.72	3.6209 (13)	152
C10—H10B···Cl2^{v}	0.99	2.65	3.6329 (13)	170

Symmetry codes: (i) $-x, -y+1, -z+1$; (ii) $-x+1, -y+2, -z+1$; (iii) $x-1, y, z$; (iv) $x, y+1, z$; (v) $-x+1, -y+1, -z+1$.

state, molecules are linear, with the central chain consisting of the methylene and ammonium fragments exhibiting an all-*trans* geometry (Fig. 2). Values of C—N—C—C and N—C—C—N torsion angles are between −172.64 (10) and 179.49 (8)°. The orientation of the phenyl rings at the two ends of the molecule differs. The C4–C9 phenyl ring is roughly perpendicular to the adjacent C—N bond and the methylene-ammonium chain. The C11–C16 ring, on the other hand, is nearly in plane with the methylene-ammonium chain. The respective torsion angles of the phenyl and methylene-ammonium planes are 89.60 (5)° for the C4–C9 ring, and 18.62 (11)° for the C11–C16. The cause for the differing torsion angles is a modulation of the phenyl rings to allow for close packing, while at the same time enabling strong N—H···Cl hydrogen bonds to be established (see *Supramolecular features* section, below).

3. Supramolecular features

The primary packing interaction that steers the arrangement of molecules in the solid state is hydrogen bonding. Ammonium H atoms form well-defined charge-assisted intermolecular N—H···Cl hydrogen bonds (Table 1), with N···Cl and H···Cl distances of around 3.08 and 2.2 Å, with close to linear N—H···Cl bond angles [168.6 (13)° or larger], as expected for strong ammonium to chloride hydrogen bonds (see Table 1 for numerical details and symmetry operators). These classical hydrogen bonds are augmented by less strong but still significant C—H···Cl interactions involving the benzylic methylene hydrogen atoms – the most acidic H atoms after the ammonium ones. Hydrogen-bond distances are longer than for the ammonium groups, C···Cl and H···Cl distances are around 3.6 and 2.6 Å, and C—H···Cl bond angles are 151 to 171°, indicating that these interactions are still directional and consolidating in nature (see Table 1 for details of individual hydrogen bonds), and they assist and augment the ammonium-to-chloride hydrogen bonds in building the larger solid-state assembly. The ethylene H atoms also feature some close H···Cl contacts, but the bond distances and especially bond angles (135° or smaller) are unfavorable, and these interactions seem to be more a result of the neighboring stronger interactions and general packing than consolidating on their own. The phenyl H atoms are not involved in directional interactions, and neither π–π stacking interactions nor strong C—H···π interactions are observed.

The NH_2^+ to Cl^- hydrogen bonds connect molecules into a set of chains along either [110] or [$\bar{1}$10] (the former at c = 0 or 1, the latter at c = 1/2). The CH_2 to Cl^- interactions involving the benzylic methylene groups then connect parallel chains with each other leading to formation of tightly hydrogen-bonded layers perpendicular to the [001] direction. The centers of the layers are made up from the hydrogen-bonded ammonium–methylene chains and the chloride anions, while the outer segments of the layers are harboring the phenyl substituents (Fig. 3). No strong interactions between parallel layers are observed, which might be one of the reasons for the strong proclivity of the crystals of *N*,*N*′-dibenzylethylenediammonium dichloride towards twinning, as we observed during screening of the material for XRD. Inversion, mirroring or twofold rotation of an entire layer does not break any bonds or attractive and directional interactions, while only moderately disturbing dispersive interactions between phenyl rings of neighboring layers, thus allowing for twinning to occur with relative ease at the interface between layers. Dominant twin relationships observed during crystal screening had been both pseudo-merohedral [twofold rotations around (100), twin matrix (1 0 0 0 −1 0 0 0−1) as well as non-merohedral [twofold around [100], twin matrix (1 0 0 0 −1 0 −0.173 0 −1)].

Within each layer, the relationship of neighboring fragments is more important. In order to not break or weaken the essential hydrogen-bonding interactions, neighboring phenyl rings need to be rotated against each other so as to allow for the ideal spacing between neighboring ammonium-methylene chains and chloride ions. Would the phenyl rings at both sides of the molecule feature the same torsion angle towards the ammonium-methylene chain, then close contacts between ortho- and meta-H atoms of adjacent phenyl rings would result, or the spacing between ammonium-methylene chain would need to widen, which would disturb and weaken the hydrogen bonds. The 89.60 (5) and 18.62 (11)° torsion angles (see molecular geometry description, above) allow for dense packing of the entire layers without either close H···H contacts or breaking of hydrogen bonds.

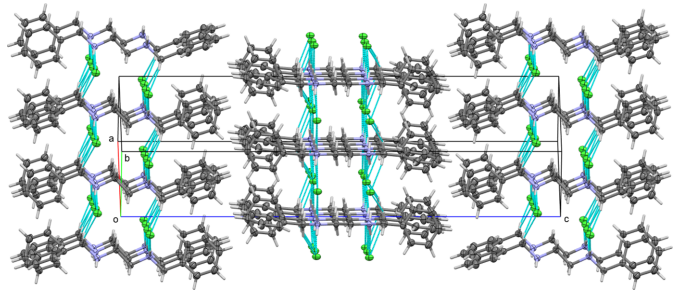

Figure 3
Packing of the title compound showing N—H···Cl and C—H···Cl hydrogen bonds, the formation of layers and modulation of the phenyl rings. View down slightly angled from [1$\bar{1}$0] (the modulation direction). 50% probability ellipsoids.

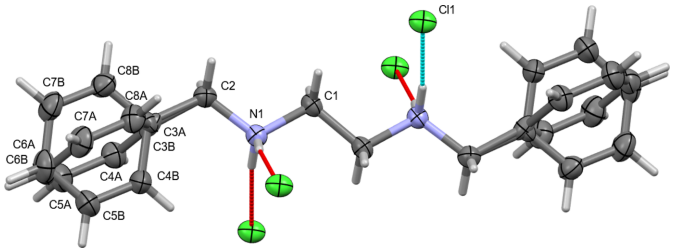

Figure 4
Hypothetical structure in *C*2/*c*. Unlabeled atoms are symmetry created (for C and N atoms: by inversion at the center of the ethylene C—C-bond).

The alternating phenyl ring rotations lead to a twofold commensurately modulated structure. The structure exhibits pseudo-translation along [110] and [$\bar{1}$10] that is exactly obeyed by the atoms of the ammonium–methylene chain as well as the *ipso* and *para* atoms of the phenyl rings, as well as the chloride ions. Ignoring *ortho* and *meta* C atoms, the structure could also be described in a monoclinic *C*-centered cell emulating space group *C*2/*c*. Refinement of the data in this setting, under omission of satellite reflections that should be absent for a *C*-centered cell, leads to a very sensical structure with half a dication in the asymmetric unit (an inversion center is located at the center of the ethylene C—C bond), and only one independent chloride ion (Fig. 4). The R_1 value is 2.90% slightly smaller than for the modulated $P2_1/n$ setting (3.25%). The phenyl rings, however, are systematically 1:1 disordered in *C*2/*c*, indicating the primitive setting to be correct. The absence of exact translational symmetry is also confirmed by the intensity data. For the dataset obtained, reflections that should be absent in the presence of exact translation have $I/\sigma(I)$ values of 4.7, while average reflections have an $I/\sigma(I)$ of 7.1. The lower symmetry, more ordered structure in $P2_1/n$ is thus the correct choice.

4. Database survey

19 Structures were identified that contain either the *N*,*N*′-dibenzylethylenediammonium dication, or *N*,*N*′-dibenzylethylenediamine as a ligand in a metal complex (Cambridge Structural Database version 5.45, November 2023; May and June 2024 updates; Groom *et al.*, 2016). The structure of the free amine is not known, and no halide salt of the dication has been reported either. Most closely related to the title compound are five salts of the dication, specifically the nitrate salt (AFIKEG; Liu *et al.*, 2007), a DMF/water solvate of the dodecakis(μ-oxido)tetradecaoxooctamolybdenum salt (OLESIJ; Talotta *et al.*, 2016), a bis(diphenylphosphinate) dihydrate (WAWVOJ; Kibardina *et al.*, 2021) and a hydroxy(oxido)oxophosphanecarboxylate (WOHBAZ; Wang *et al.*, 2019) and the tetrachlorocopper(II) salt (ZUSYEU; Liu *et al.*, 2020). Three of these exhibit an all-*trans* geometry of the methylene–ammonium chain with both phenyl groups perpendicular to the plane of the chain (the conformation expected to be the most stable in the absence of packing forces). WOHBAZ and OLESIJ feature each one *gauche* angle in the methylene–ammonium chain. No structures involving the monocation are reported (p*K*a values of the two amino groups are expected to be uncorrelated and essentially the same). 14 metal complexes (and two duplicate structures) of the neutral amine are reported, with metal ions comprising first row transition metals (Mn, Co, Cu, Ni, Zn) as well as Ru. All metal complexes feature a chelating ligand coordinated *via* both nitrogen atoms to the same metal ion. Both *trans* and *cis* arrangements of the N—H (or N—Ph) groups are observed.

Table 2
Experimental details.

Crystal data	
Chemical formula	$C_{16}H_{22}N_2^{2+}\cdot 2Cl^-$
M_r	313.25
Crystal system, space group	Monoclinic, $P2_1/n$
Temperature (K)	150
a, b, c (Å)	7.1738 (4), 7.2872 (4), 32.0348 (18)
β (°)	91.111 (2)
V (Å^3)	1674.37 (16)
Z	4
Radiation type	Cu $K\alpha$
μ (mm^{-1})	3.41
Crystal size (mm)	0.19 × 0.18 × 0.12
Data collection	
Diffractometer	Bruker AXS D8 Quest
Absorption correction	Multi-scan (*SADABS*; Krause *et al.*, 2015)
T_{min}, T_{max}	0.565, 0.754
No. of measured, independent and observed [$I > 2\sigma(I)$] reflections	38723, 3643, 3295
R_{int}	0.059
(sin $\theta/\lambda)_{max}$ (Å^{-1})	0.640
Refinement	
$R[F^2 > 2\sigma(F^2)]$, $wR(F^2)$, S	0.033, 0.095, 1.08
No. of reflections	3643
No. of parameters	194
H-atom treatment	H atoms treated by a mixture of independent and constrained refinement
$\Delta\rho_{max}$, $\Delta\rho_{min}$ (e Å^{-3})	0.34, −0.19

Computer programs: *APEX4* and *SAINT* (Bruker, 2022), *SHELXT* (Sheldrick, 2015*a*), *SHELXL2019/2* (Sheldrick, 2015*b*), *ShelXle* Rev1580 (Hübschle *et al.*, 2011) and *Mercury* (Macrae *et al.*, 2020).

5. Synthesis and crystallization

After the addition of benzoic acid (0.5 g, 4.1 mmol) and 1,2-dichloroethane (40 mL, 506 mmol, 123 equiv) to a 100 mL round-bottomed flask, both triethylamine (1.1 mL, 7.9 mmol, 2 equiv) and diphenylphosphoryl azide (1.1 mL, 5.1 mmol, 1.2 equiv) were added at room temperature *via* syringe. The reaction mixture was placed under a blanket of Ar and allowed to stir at room temperature for 4 h at which time benzylamine (1.8 mL, 16.5 mmol, 4 equiv) was added *via* syringe. Upon addition of the amine, the reaction mixture was externally heated to reflux and held at reflux overnight (17h). After allowing the reaction mixture to cool to room temperature, the observed solid was isolated by vacuum filtration. The material was next transferred to a small beaker and triturated using cold 1,2-dichloroethane (5.0 mL). The isolated material after a second filtration and removal of the volatiles *in vacuo* was 350 mg [1.1 mmol (7% yield using

benzyl amine as limiting reactant)]; white solid; m.p. 565–569 K (dec).

IR (neat, ATR) cm^{-1}: 3650 (*w*), 3057 (*m*), 3032 (*m*), 2748 (*s*), 2689 (*s*), 2421 (*s*), 1455 (*s*), 1026 (*s*). ^{1}H NMR (DMSO-d_6, 500 MHz): δ 9.68 (*br s*, 4H), 7.58–7.57 (*m*, 4H), 7.46–7.41 (*m*, 6H), 4.19 (*s*, 4H), 3.35 (*s*, 4H). ^{13}C NMR (DMSO-d_6, 125 MHz): δ 131.8, 130.0, 129.0, 127.8, 50.2, 42.7. Spectroscopic data agree with the literature (Asadi *et al.*, 2005).

From this sample, 82 mg were subjected to crystallization by vapor diffusion. A 10 mL beaker containing the material dissolved in 3.5 mL of deionized water was placed inside a 250 mL chamber filled with approximately 100 mL of 95% ethanol. Intergrown plates and flakes formed after 24 h. Crystals were taken directly from mother liquor, dispersed in a small amount of Fomblin oil, investigated using a polarized light microscope and selected crystals were mounted onto a MiTeGen micromesh mount for crystal screening and XRD data collection.

6. Refinement

Crystal data, data collection and structure refinement details are summarized in Table 2. H atoms attached to carbon atoms were positioned geometrically and constrained to ride on their parent atoms. C—H bond distances were constrained to 0.95 Å for aromatic and to 0.99 Å for CH_2 moieties, respectively. Positions of ammonium H atoms were freely refined. U_{iso}(H) values were set to 1.2 times U_{eq}(C/N).

Acknowledgements

BNB, MHM, and DCF would like to thank the Department of Chemistry, Honors College, Office of Undergraduate Research, and University of South Alabama Foundation for their generous financial support of undergraduate research.

Funding information

Funding for this research was provided by: Department of Chemistry; Honors College, University of South Alabama's Office of Undergraduate Research (grant to DCF); National Science Foundation, Directorate for Mathematical and Physical Sciences (award No. CHE 1625543); The College of Science, Purdue University, 2020 and 2023 Laboratory and University Core Facility Research Equipment Programs (grant No. 2020, 2023).

References

Asadi, H., Golchoubia, H. & Welter, R. (2005). *J. Mol. Struct.* **779**, 30–37.
Brownell, S. E. & Kloser, M. J. (2015). *Stud. High. Educ.* **40**, 525–544.
Bruker (2022). *APEX4* and *SAINT*. Bruker AXS Inc. Madison, Wisconsin, USA.
Curtius, T. (1890). *Ber. Deutsch. Chem. Ges. zu Berlin*, **23**(2), 3023–3033.
Curtius, T. (1894). *J. Prakt. Chem.* **50**, 275–294.
Ghosh, A. K., Brindisi, M. & Sarkar, A. (2018). *ChemMedChem*, **13**, 2351–2373.
Groom, C. R., Bruno, I. J., Lightfoot, M. P. & Ward, S. C. (2016). *Acta Cryst.* B**72**, 171–179.
Hou, X., Zaks, T., Langer, R. & Dong, Y. (2021). *Nat. Rev. Mater.* **6**, 1078–1094.
Hübschle, C. B., Sheldrick, G. M. & Dittrich, B. (2011). *J. Appl. Cryst.* **44**, 1281–1284.
Kibardina, L. K., Trifonov, A. V., Dobrynin, A. B., Pudovik, M. A. & Burilov, A. R. (2021). *Zh. Obshch. Khim. (Russ. J. Gen. Chem.)*, **91**, 1667–1673.
Krause, L., Herbst-Irmer, R., Sheldrick, G. M. & Stalke, D. (2015). *J. Appl. Cryst.* **48**, 3–10.
Liu, C., Zhang, W. & Cai, G. (2020). *Crystals*, **10**, 528.
Liu, Y.-F., Xia, H.-T., Wang, D.-Q., Yang, S.-P. & Meng, Y.-L. (2007). *Acta Cryst.* E**63**, o3836.
Macrae, C. F., Sovago, I., Cottrell, S. J., Galek, P. T. A., McCabe, P., Pidcock, E., Platings, M., Shields, G. P., Stevens, J. S., Towler, M. & Wood, P. A. (2020). *J. Appl. Cryst.* **53**, 226–235.
Ninomiya, K., Shioiri, T. & Yamada, S. (1974). *Tetrahedron*, **30**, 2151–2157.
Reddy, B. N., Reddy, P. V. G., Reddy, P. S., Reddy, S. M., Reddy, S. R. S. & Pathak, M. (2015). *Synth. Commun.* **45**, 831–837.
Sheldrick, G. M. (2015*a*). *Acta Cryst.* A**71**, 3–8.
Sheldrick, G. M. (2015*b*). *Acta Cryst.* C**71**, 3–8.
Talotta, C., Rubino, L., Gaeta, C., Capitelli, F., Saviano, M., Brancatelli, G., Geremia, S., Vasca, E. & Neri, P. (2016). *Supramol. Chem.* **28**, 403–417.
Wang, J., Tao, Y., Feng, J., Niu, Y., Liu, J. & Huang, Y. (2019). *RSC Adv.* **9**, 21318–21322.
Watts, F. M. & Rodriguez, J. G. (2023). *J. Chem. Educ.* **100**, 3261–3275.

supporting information

Acta Cryst. (2024). E**80**, 1130-1134 [https://doi.org/10.1107/S205698902400954X]

N,*N*′-Dibenzylethylenediammonium dichloride

Mary Helene Marmande, Bailey N. Baxter, Matthias Zeller and David C. Forbes

Computing details

Benzyl[2-(benzylazaniumyl)ethyl]azanium dichloride

Crystal data

$C_{16}H_{22}N_2^{2+}\cdot 2Cl^-$
M_r = 313.25
Monoclinic, $P2_1/n$
a = 7.1738 (4) Å
b = 7.2872 (4) Å
c = 32.0348 (18) Å
β = 91.111 (2)°
V = 1674.37 (16) Å^3
Z = 4
$F(000)$ = 664
D_x = 1.243 Mg m^{-3}
Cu $K\alpha$ radiation, λ = 1.54178 Å
Cell parameters from 9984 reflections
θ = 5.5–80.0°
μ = 3.41 mm^{-1}
T = 150 K
Block, colourless
0.19 × 0.18 × 0.12 mm

Data collection

Bruker AXS D8 Quest diffractometer
Radiation source: I-mu-S 3.0 microsource X-ray tube
HELIOS multilayer Montel optics monochromator
Detector resolution: 7.4074 pixels mm^{-1}
ω and phi scans
Absorption correction: multi-scan (SADABS; Krause *et al.*, 2015)
T_{min} = 0.565, T_{max} = 0.754
38723 measured reflections
3643 independent reflections
3295 reflections with $I > 2\sigma(I)$
R_{int} = 0.059
θ_{max} = 80.4°, θ_{min} = 2.8°
h = −9→9
k = −8→9
l = −40→40

Refinement

Refinement on F^2
Least-squares matrix: full
$R[F^2 > 2\sigma(F^2)]$ = 0.033
$wR(F^2)$ = 0.095
S = 1.08
3643 reflections
194 parameters
0 restraints
Primary atom site location: dual
Secondary atom site location: difference Fourier map
Hydrogen site location: mixed
H atoms treated by a mixture of independent and constrained refinement
$w = 1/[\sigma^2(F_o^2) + (0.0421P)^2 + 0.4315P]$ where $P = (F_o^2 + 2F_c^2)/3$
$(\Delta/\sigma)_{max}$ = 0.002
$\Delta\rho_{max}$ = 0.34 e Å^{-3}
$\Delta\rho_{min}$ = −0.19 e Å^{-3}
Extinction correction: *SHELXL2019/2* (Sheldrick, 2015b), $Fc^*=kFc[1+0.001xFc^2\lambda^3/\sin(2\theta)]^{-1/4}$
Extinction coefficient: 0.0023 (3)

Special details

Geometry. All esds (except the esd in the dihedral angle between two l.s. planes) are estimated using the full covariance matrix. The cell esds are taken into account individually in the estimation of esds in distances, angles and torsion angles; correlations between esds in cell parameters are only used when they are defined by crystal symmetry. An approximate (isotropic) treatment of cell esds is used for estimating esds involving l.s. planes.

Fractional atomic coordinates and isotropic or equivalent isotropic displacement parameters (Å²)

	x	*y*	*z*	U_{iso}*/U_{eq}
Cl1	0.67834 (4)	0.83178 (4)	0.55982 (2)	0.03137 (12)
Cl2	0.17299 (4)	0.32743 (4)	0.55905 (2)	0.03030 (11)
N1	0.26034 (13)	0.74282 (13)	0.55869 (3)	0.0239 (2)
H1C	0.383 (2)	0.758 (2)	0.5622 (4)	0.029*
H1D	0.231 (2)	0.622 (2)	0.5611 (4)	0.029*
N2	0.24797 (13)	0.75055 (13)	0.44089 (3)	0.0227 (2)
H2C	0.129 (2)	0.732 (2)	0.4382 (4)	0.027*
H2D	0.273 (2)	0.868 (2)	0.4385 (4)	0.027*
C1	0.20364 (17)	0.80213 (16)	0.51580 (3)	0.0266 (2)
H1A	0.231807	0.934128	0.512218	0.032*
H1B	0.067652	0.784755	0.511695	0.032*
C2	0.30762 (16)	0.69063 (16)	0.48356 (3)	0.0262 (2)
H2A	0.443622	0.708939	0.487384	0.031*
H2B	0.280311	0.558490	0.487189	0.031*
C3	0.16624 (18)	0.85318 (17)	0.59161 (4)	0.0297 (3)
H3A	0.029932	0.851445	0.586173	0.036*
H3B	0.208683	0.982172	0.589849	0.036*
C4	0.20589 (16)	0.78214 (17)	0.63501 (4)	0.0274 (2)
C5	0.08951 (19)	0.65189 (19)	0.65256 (4)	0.0374 (3)
H5	−0.012124	0.603728	0.636570	0.045*
C6	0.1203 (2)	0.5915 (2)	0.69321 (4)	0.0439 (3)
H6	0.040482	0.501694	0.704820	0.053*
C7	0.2665 (2)	0.6616 (2)	0.71675 (4)	0.0438 (4)
H7	0.286901	0.621077	0.744657	0.053*
C8	0.3829 (2)	0.7903 (2)	0.69975 (4)	0.0435 (3)
H8	0.483795	0.838448	0.715983	0.052*
C9	0.35393 (18)	0.85042 (18)	0.65893 (4)	0.0357 (3)
H9	0.435684	0.938554	0.647356	0.043*
C10	0.34086 (17)	0.64365 (17)	0.40769 (4)	0.0281 (3)
H10A	0.298227	0.514629	0.409097	0.034*
H10B	0.477090	0.644637	0.413258	0.034*
C11	0.30333 (16)	0.71545 (16)	0.36427 (3)	0.0259 (2)
C12	0.15397 (19)	0.82726 (19)	0.35336 (4)	0.0378 (3)
H12	0.067446	0.862173	0.373986	0.045*
C13	0.1293 (2)	0.8890 (2)	0.31248 (4)	0.0433 (3)
H13	0.028142	0.968187	0.305545	0.052*
C14	0.2514 (2)	0.83566 (19)	0.28202 (4)	0.0406 (3)
H14	0.234239	0.877038	0.254083	0.049*
C15	0.3986 (2)	0.7217 (2)	0.29246 (4)	0.0441 (3)

H15	0.481997	0.683011	0.271523	0.053*
C16	0.42558 (19)	0.66346 (18)	0.33326 (4)	0.0374 (3)
H16	0.528917	0.586997	0.340157	0.045*

Atomic displacement parameters (Å²)

	U^{11}	U^{22}	U^{33}	U^{12}	U^{13}	U^{23}
Cl1	0.02593 (17)	0.02588 (17)	0.04219 (19)	−0.00401 (9)	−0.00181 (12)	0.00266 (10)
Cl2	0.02475 (17)	0.02573 (17)	0.04041 (19)	−0.00358 (9)	0.00017 (12)	0.00231 (10)
N1	0.0237 (5)	0.0238 (5)	0.0242 (5)	−0.0018 (4)	−0.0004 (3)	0.0014 (4)
N2	0.0218 (5)	0.0231 (5)	0.0233 (4)	−0.0013 (3)	−0.0007 (3)	0.0017 (3)
C1	0.0285 (6)	0.0277 (5)	0.0235 (5)	0.0010 (4)	−0.0020 (4)	0.0033 (4)
C2	0.0274 (6)	0.0275 (6)	0.0236 (5)	0.0012 (4)	−0.0023 (4)	0.0035 (4)
C3	0.0312 (6)	0.0297 (6)	0.0282 (6)	0.0044 (5)	0.0018 (5)	0.0005 (4)
C4	0.0299 (6)	0.0269 (5)	0.0257 (5)	0.0027 (4)	0.0029 (4)	−0.0018 (4)
C5	0.0364 (7)	0.0419 (7)	0.0339 (6)	−0.0082 (5)	0.0040 (5)	−0.0021 (5)
C6	0.0529 (8)	0.0429 (8)	0.0363 (7)	−0.0040 (6)	0.0138 (6)	0.0053 (6)
C7	0.0571 (9)	0.0500 (9)	0.0245 (6)	0.0146 (6)	0.0042 (6)	0.0010 (5)
C8	0.0460 (8)	0.0492 (8)	0.0348 (7)	0.0014 (6)	−0.0092 (6)	−0.0074 (6)
C9	0.0368 (7)	0.0344 (6)	0.0359 (6)	−0.0052 (5)	−0.0006 (5)	−0.0016 (5)
C10	0.0287 (6)	0.0294 (6)	0.0263 (6)	0.0046 (4)	−0.0001 (4)	0.0001 (4)
C11	0.0285 (5)	0.0240 (5)	0.0252 (5)	−0.0034 (4)	0.0008 (4)	−0.0009 (4)
C12	0.0383 (7)	0.0492 (8)	0.0259 (6)	0.0125 (5)	0.0008 (5)	−0.0003 (5)
C13	0.0485 (8)	0.0514 (8)	0.0298 (6)	0.0120 (6)	−0.0055 (5)	0.0026 (6)
C14	0.0539 (8)	0.0429 (8)	0.0250 (6)	−0.0064 (6)	−0.0003 (5)	0.0030 (5)
C15	0.0526 (8)	0.0476 (8)	0.0326 (7)	0.0010 (6)	0.0153 (6)	−0.0005 (6)
C16	0.0381 (7)	0.0389 (7)	0.0357 (7)	0.0055 (5)	0.0094 (5)	0.0019 (5)

Geometric parameters (Å, º)

N1—C1	1.4894 (14)	C6—H6	0.9500
N1—C3	1.4974 (15)	C7—C8	1.375 (2)
N1—H1C	0.893 (16)	C7—H7	0.9500
N1—H1D	0.908 (17)	C8—C9	1.3907 (19)
N2—C10	1.4864 (15)	C8—H8	0.9500
N2—C2	1.4897 (14)	C9—H9	0.9500
N2—H2C	0.867 (16)	C10—C11	1.5057 (16)
N2—H2D	0.881 (17)	C10—H10A	0.9900
C1—C2	1.5211 (18)	C10—H10B	0.9900
C1—H1A	0.9900	C11—C12	1.3854 (17)
C1—H1B	0.9900	C11—C16	1.3905 (17)
C2—H2A	0.9900	C12—C13	1.3930 (18)
C2—H2B	0.9900	C12—H12	0.9500
C3—C4	1.5056 (16)	C13—C14	1.380 (2)
C3—H3A	0.9900	C13—H13	0.9500
C3—H3B	0.9900	C14—C15	1.379 (2)
C4—C9	1.3897 (17)	C14—H14	0.9500
C4—C5	1.3899 (17)	C15—C16	1.3843 (19)

C5—C6	1.3885 (19)	C15—H15	0.9500
C5—H5	0.9500	C16—H16	0.9500
C6—C7	1.378 (2)		
C1—N1—C3	112.03 (9)	C7—C6—C5	120.09 (13)
C1—N1—H1C	109.3 (9)	C7—C6—H6	120.0
C3—N1—H1C	107.5 (10)	C5—C6—H6	120.0
C1—N1—H1D	107.5 (9)	C8—C7—C6	119.84 (13)
C3—N1—H1D	110.5 (9)	C8—C7—H7	120.1
H1C—N1—H1D	110.1 (14)	C6—C7—H7	120.1
C10—N2—C2	112.21 (9)	C7—C8—C9	120.42 (13)
C10—N2—H2C	107.5 (10)	C7—C8—H8	119.8
C2—N2—H2C	108.1 (10)	C9—C8—H8	119.8
C10—N2—H2D	110.6 (9)	C4—C9—C8	120.29 (12)
C2—N2—H2D	108.0 (9)	C4—C9—H9	119.9
H2C—N2—H2D	110.3 (14)	C8—C9—H9	119.9
N1—C1—C2	110.04 (10)	N2—C10—C11	113.85 (9)
N1—C1—H1A	109.7	N2—C10—H10A	108.8
C2—C1—H1A	109.7	C11—C10—H10A	108.8
N1—C1—H1B	109.7	N2—C10—H10B	108.8
C2—C1—H1B	109.7	C11—C10—H10B	108.8
H1A—C1—H1B	108.2	H10A—C10—H10B	107.7
N2—C2—C1	109.31 (10)	C12—C11—C16	118.39 (11)
N2—C2—H2A	109.8	C12—C11—C10	124.12 (10)
C1—C2—H2A	109.8	C16—C11—C10	117.48 (11)
N2—C2—H2B	109.8	C11—C12—C13	120.71 (12)
C1—C2—H2B	109.8	C11—C12—H12	119.6
H2A—C2—H2B	108.3	C13—C12—H12	119.6
N1—C3—C4	112.71 (9)	C14—C13—C12	120.20 (13)
N1—C3—H3A	109.1	C14—C13—H13	119.9
C4—C3—H3A	109.1	C12—C13—H13	119.9
N1—C3—H3B	109.1	C15—C14—C13	119.45 (13)
C4—C3—H3B	109.1	C15—C14—H14	120.3
H3A—C3—H3B	107.8	C13—C14—H14	120.3
C9—C4—C5	118.70 (11)	C14—C15—C16	120.39 (12)
C9—C4—C3	120.98 (11)	C14—C15—H15	119.8
C5—C4—C3	120.26 (11)	C16—C15—H15	119.8
C6—C5—C4	120.65 (12)	C15—C16—C11	120.83 (12)
C6—C5—H5	119.7	C15—C16—H16	119.6
C4—C5—H5	119.7	C11—C16—H16	119.6
C3—N1—C1—C2	178.09 (11)	C7—C8—C9—C4	0.6 (2)
C10—N2—C2—C1	−178.55 (11)	C2—N2—C10—C11	−172.64 (10)
N1—C1—C2—N2	179.49 (8)	N2—C10—C11—C12	−20.36 (17)
C1—N1—C3—C4	173.85 (10)	N2—C10—C11—C16	160.55 (11)
N1—C3—C4—C9	92.30 (14)	C16—C11—C12—C13	−1.3 (2)
N1—C3—C4—C5	−90.43 (14)	C10—C11—C12—C13	179.62 (13)
C9—C4—C5—C6	0.14 (19)	C11—C12—C13—C14	1.6 (2)

C3—C4—C5—C6	−177.19 (12)	C12—C13—C14—C15	−0.4 (2)
C4—C5—C6—C7	0.5 (2)	C13—C14—C15—C16	−1.0 (2)
C5—C6—C7—C8	−0.6 (2)	C14—C15—C16—C11	1.3 (2)
C6—C7—C8—C9	0.1 (2)	C12—C11—C16—C15	−0.1 (2)
C5—C4—C9—C8	−0.66 (19)	C10—C11—C16—C15	179.03 (12)
C3—C4—C9—C8	176.65 (12)		

Hydrogen-bond geometry (Å, º)

D—H···*A*	*D*—H	H···*A*	*D*···*A*	*D*—H···*A*
N1—H1*C*···Cl1	0.893 (16)	2.187 (16)	3.0675 (10)	168.6 (13)
N1—H1*D*···Cl2	0.908 (17)	2.189 (17)	3.0913 (10)	172.7 (13)
N2—H2*C*···Cl2^{i}	0.867 (16)	2.213 (16)	3.0730 (10)	171.7 (13)
N2—H2*D*···Cl1^{ii}	0.881 (17)	2.213 (17)	3.0893 (10)	172.9 (13)
C1—H1*A*···Cl1^{ii}	0.99	2.95	3.7125 (12)	135
C1—H1*B*···Cl2^{i}	0.99	2.94	3.7000 (12)	135
C2—H2*A*···Cl1	0.99	2.98	3.7213 (12)	133
C2—H2*B*···Cl2	0.99	2.97	3.7251 (12)	134
C3—H3*A*···Cl1^{iii}	0.99	2.65	3.6296 (13)	171
C3—H3*B*···Cl2^{iv}	0.99	2.71	3.6106 (13)	151
C10—H10*A*···Cl1^{v}	0.99	2.72	3.6209 (13)	152
C10—H10*B*···Cl2^{v}	0.99	2.65	3.6329 (13)	170

Symmetry codes: (i) −*x*, −*y*+1, −*z*+1; (ii) −*x*+1, −*y*+2, −*z*+1; (iii) *x*−1, *y*, *z*; (iv) *x*, *y*+1, *z*; (v) −*x*+1, −*y*+1, −*z*+1.